Measurement of the CP violation phase ϕ_s in $B_s^0 \rightarrow J/\psi\phi$ decay in ATLAS using 80.5 fb^{-1} of LHC data at 13 TeV

On behalf of ATLAS Collaboration

31 August - 11 September 2019

Workshop on Connecting Insights in Fundamental Physics: Standard Model and Beyond

Corfu 2019

Motivation

- Interference of direct decay and decay with mixing into the same final state of $B_s^0 \to J/\psi\phi$ gives rise to time-dependent CP violation (CPV)

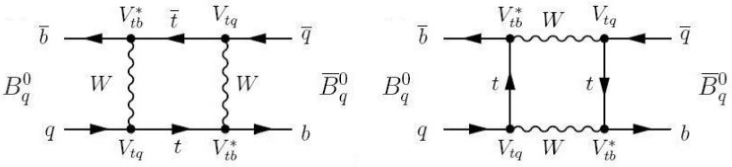

- CPV phase ϕ_s is the weak phase difference between the $B_s^0 - \bar{B}_s^0$ mixing amplitude and the direct $b \to c\bar{c}s$ decay amplitude
- In the Standard Model (SM) the ϕ_s is related to the CKM matrix and is small:

$$\phi_s \simeq -2\beta_s = -2arg\frac{V_{ts}V_{tb}^*}{V_{cs}V_{cb}^*} = -0.0363^{+0.0016}_{-0.0015}\ \mathrm{rad}$$

- New Physics (NP) processes could contribute to the mixing box diagrams, potentially allowing for large deviations in ϕ_s from the SM prediction

- Alongside ϕ_s, other quantities are describing the differential decay rate:
  - Decay widths and masses of the two mass eigenstates
  - CP even/odd state amplitudes and phases

Experimental Status after LHC Run1: CPV in $B_s^0 \to J/\psi\phi$

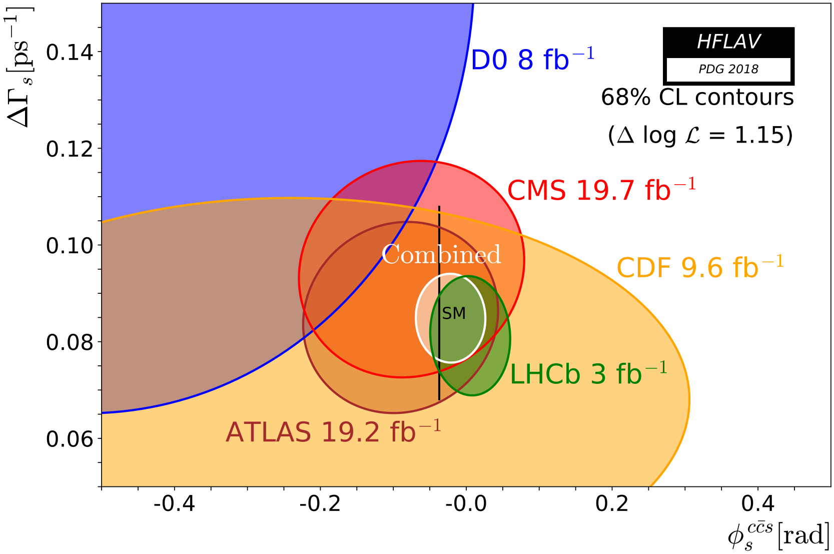

- LHC Run 1 results consistent with the Standard Model prediction
- Search for New Physics needs increase of the ϕ_s precision

Data and Monte Carlo simulation samples

Run 2 Data:

- $4.9\ \mathrm{fb}^{-1}$ of $13\ \mathrm{TeV}$ pp collision data in 2015
- $31.3\ \mathrm{fb}^{-1}$ of $13\ \mathrm{TeV}$ pp collision data in 2016
- $44.3\ \mathrm{fb}^{-1}$ of $13\ \mathrm{TeV}$ pp collision data in 2017
- Events collected with mixture of triggers based on $J/\psi \to \mu^+\mu^-$ identification, with muon p_{T} thresholds of either $4\ \mathrm{GeV}$ or $6\ \mathrm{GeV}$ (vary over run periods)

MC samples:

- MC samples for $B_s^0 \to J/\psi\phi$
- MC samples for peaking backgrounds $B_d^0 \to J/\psi K^{*0}$, $B_d^0 \to J/\psi K\pi$ and $\Lambda_b^0 \to J/\psi Kp$
- MC samples for tagging calibration channel $B^\pm \to J/\psi K^\pm$ (systematics and cross-checks only, real data used for calibration)

Reconstruction and candidate selection

Event

- Triggers (previous slide) and Good Data Quality selection criteria
- At least one PV formed from at least 4 ID tracks
- At least one pair of ID+MS identified $\mu^+\mu^-$

$J/\psi \to \mu^+\mu^-$

- Dimuon vertex fit $\chi^2/\mathrm{d.o.f.} < 10$
- Three dimuon invariant mass windows for BB/BE/EE (barrel, endcap) muon combinations

$\phi \to K^+K^-$

- $p_\mathrm{T}(K) > 1\ \mathrm{GeV}$
- $1008.5\ \mathrm{MeV} < m(KK) < 1030.5\ \mathrm{MeV}$

$B_s^0 \to J/\psi(\mu^+\mu^-)\phi(K^+K^-)$

- $p_\mathrm{T}(B_s^0) > 10\ \mathrm{GeV}$
- Four-track vertex fit $\chi^2/\mathrm{d.o.f.} < 3$ (J/ψ mass constrained)
- Keep only the candidate with best vertex fit $\chi^2/\mathrm{d.o.f.}$ in event
- $5150\ \mathrm{MeV} < m(B_s^0) < 5650\ \mathrm{MeV} \to$ **in total 3 210 429 B_s^0 candidates**

Angular analysis

- $B_s^0 \to J/\psi\phi$ decay $=$ decay of pseudoscalar to vector-vector
- Final state: admixture of CP-odd ($L = 1$) and CP-even ($L = 0, 2$) states
- Distinguishable through time-dependent angular analysis
- Non-resonant S-wave decay $B_s^0 \to J/\psi K^+K^-$ contribute to the final state and is included in the differential decay rate due to interference with the signal $B_s^0 \to J/\psi(\mu^+\mu^-)\phi(K^+K^-)$ decay

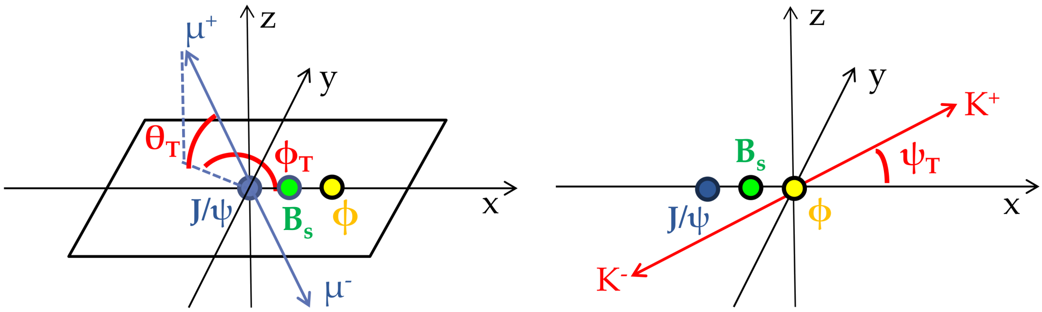

Figure: Angles between final state particles in transversity basis

Mass-lifetime-angular fit

We perform unbinned maximum likelihood fit simultaneously for B_s^0 mass, decay time and the decay angles:

$$
\begin{aligned}
\ln \mathcal{L} = \sum_{i=1}^{N} \{ w_i \cdot \ln(f_\mathrm{s} \cdot \mathcal{F}_\mathrm{s}(m_i, t_i, \sigma_{m_i}, \sigma_{t_i}, \Omega_i, P(B|Q), p_{\mathrm{T}_i}) \\
+ f_\mathrm{s} \cdot f_{B^0} \cdot \mathcal{F}_{B^0}(m_i, t_i, \sigma_{m_i}, \sigma_{t_i}, \Omega_i, P(B|Q), p_{\mathrm{T}_i}) \\
+ f_\mathrm{s} \cdot f_{\Lambda_b} \cdot \mathcal{F}_{\Lambda_b}(m_i, t_i, \sigma_{m_i}, \sigma_{t_i}, \Omega_i, P(B|Q), p_{\mathrm{T}_i}) \\
+ (1 - f_\mathrm{s} \cdot (1 + f_{B^0} + f_{\Lambda_b})) \mathcal{F}_\mathrm{bkg}(m_i, t_i, \sigma_{m_i}, \sigma_{t_i}, \Omega_i, P(B|Q), p_{\mathrm{T}_i}) \}
\end{aligned}
$$

Physics parameters

- CPV phase: ϕ_s
- Decay widths: $\Delta\Gamma_s$, Γ_s
- Decay amplitudes: $|A_0(0)|^2$, $|A_{||}(0)|^2$, $\delta_{||}$, $\delta_\perp$
- S-wave: $|A_S(0)|^2$, δ_S
- Δm_s fixed to PDG

Observables

- Base observables: m_i, t_i, Ω_i
- Conditional observables per-candidate:
  - resolutions: σ_{m_i}, σ_{t_i} (B-p_{T_i} dependent)
  - tagging probability and method: $P(B|Q)$
  - Corresponding "Punzi" distributions for signal and combinatorial background are extracted from data using sidebands subtraction (the PDFs shapes are then fixed in the fit)

Flavour tagging overview

Opposite side tagging

- Use b-$\bar{b}$ correlation to determine initial signal flavour from the other B-meson in the event
  - $b \to l$ transition are clean tagging method
  - $b \to c \to l$ and neutral B-meson oscillations dilute the tagging
- Provide probability $P(B|Q)$ of signal candidate to be B_s^0 or $\bar{B}_s^0$

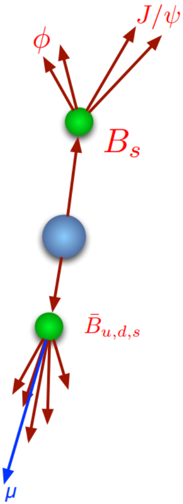

Tagger types

- tight muon, low-p_{T} muon, electron, b-tagged jet

- Signal flavour probability derived from charge of p_{T} weighted tracks in a cone around the opposite side primary object ($e^{\pm}$, $\mu^{\pm}$, b-jet)

$$Q_x = \frac{\sum_i^{N \text{ tracks}} q_i \cdot (p_{\mathrm{T}i})^{\kappa}}{\sum_i^{N \text{ tracks}} (p_{\mathrm{T}i})^{\kappa}}$$

- Search order based on best purity:
  tight muons, electrons, low-p_{T} muons, b-jets

Tagging calibration

Calibration using $B^{\pm} \to J/\psi K^{\pm}$ events (real data)

- Self-tagging non-oscillating channel
- Dimuon candidates in range $2.8 < m(\mu\mu) < 3.4\ \mathrm{GeV}$
- $p_{\mathrm{T}}(\mu) > 4\ \mathrm{GeV}$, $p_{\mathrm{T}}(K^{\pm}) > 1\ \mathrm{GeV}$
- Invariant mass in range $5.0 < m(\mu\mu K^{\pm}) < 5.6\ \mathrm{GeV}$
- $\tau(B^{\pm}) > 0.2\ \mathrm{ps}^{-1}$ reducing prompt combinatorial background

Tagging performance

- Efficiency $\epsilon = N_{\mathrm{tagged}}/N_{\mathrm{Bcand.}}$ (fraction of tagged signals)
- Dilution $D = (1 - 2w)$ (w is miss-tag probability)
- Tagging power $TP = \epsilon D^2$ (figure of merit of tagger performance)

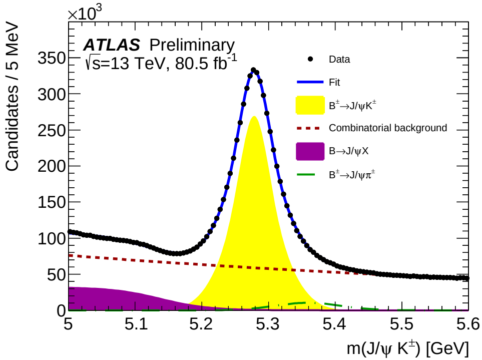

Tagging performance

- Tagging performance in the $B^{\pm}$ channel

Tagger	Efficiency [%]	Dilution [%]	Tagging Power [%]
Tight μ	4.50 ± 0.01	43.8 ± 0.2	0.862 ± 0.009
Low-p_{T} μ	3.12 ± 0.01	29.9 ± 0.2	0.278 ± 0.006
Electron	1.57 ± 0.01	41.8 ± 0.2	0.274 ± 0.004
Jet-charge	5.54 ± 0.01	20.4 ± 0.1	0.231 ± 0.005
Total	14.74 ± 0.02	33.4 ± 0.1	1.65 ± 0.01

- Tag charge distribution and calibration curve for tight muons (for discrete part and continious part)

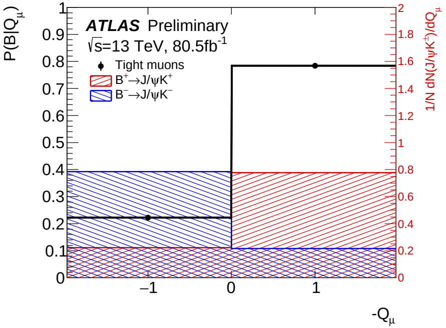

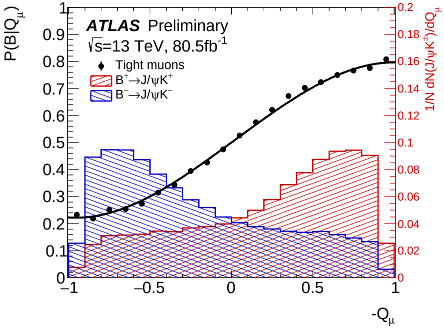

Projections of the mass-lifetime-angular fit

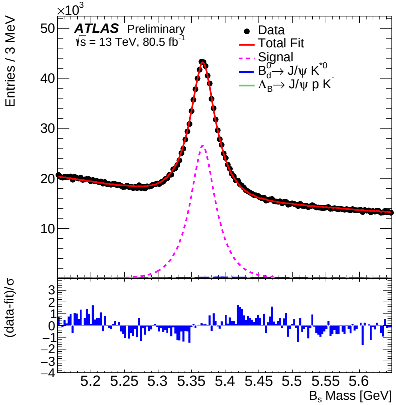

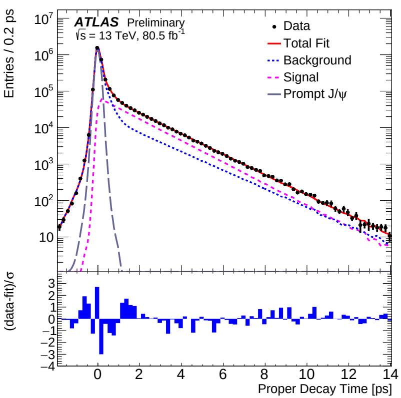

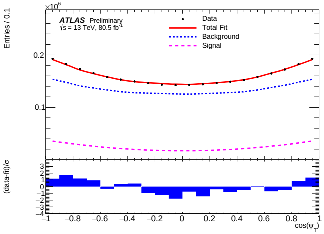

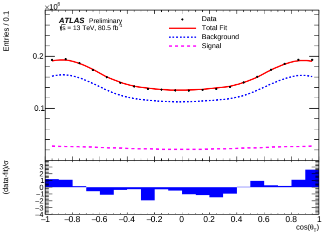

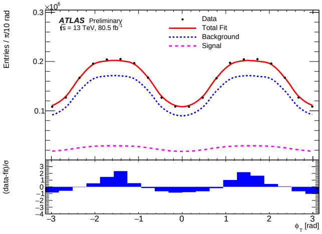

- Pull plots include both statistical and systematical uncertainties

Results of the mass-lifetime-angular fit

Parameter	Value	Statistical uncertainty	Systematic uncertainty
ϕ_s[rad]	-0.068	0.038	0.018
$\Delta\Gamma_s$[ps^{-1}]	0.067	0.005	0.002
Γ_s[ps^{-1}]	0.669	0.001	0.001
$\lvert A_{\parallel}(0)\rvert^2$	0.219	0.002	0.002
$\lvert A_0(0)\rvert^2$	0.517	0.001	0.004
$\lvert A_S(0)\rvert^2$	0.046	0.003	0.004
$\delta_\perp$ [rad]	2.946	0.101	0.097
$\delta_\parallel$ [rad]	3.267	0.082	0.201
$\delta_\perp - \delta_S$ [rad]	-0.220	0.037	0.010

	$\Delta\Gamma$	Γ_s	$\lvert A_{\parallel}(0)\rvert^2$	$\lvert A_0(0)\rvert^2$	$\lvert A_S(0)\rvert^2$	$\delta_\parallel$	$\delta_\perp$	$\delta_\perp - \delta_S$
ϕ_s	-0.111	0.038	0.000	-0.008	-0.015	0.019	-0.001	-0.011
$\Delta\Gamma$	1	-0.563	0.092	0.097	0.042	0.036	0.011	0.009
Γ_s		1	-0.139	-0.040	0.103	-0.105	-0.041	0.016
$\lvert A_{\parallel}(0)\rvert^2$			1	-0.349	-0.216	0.571	0.223	-0.035
$\lvert A_0(0)\rvert^2$				1	0.299	-0.129	-0.056	0.051
$\lvert A_S(0)\rvert^2$					1	-0.408	-0.175	0.164
$\delta_\parallel$						1	0.392	-0.041
$\delta_\perp$							1	0.052

Systematic uncertainties

- Systematics assumed uncorrelated → $\mathrm{Total} = \sqrt{\sum_i \mathrm{syst}_i^2}$
- Tagging systematics dominant for ϕ_s
  - Accounting for pile-up dependence, calibration curves model and MC precision, "Punzi" PDFs variations, difference between $B^{\pm}$ and B_s^0 kinematics
- Fit-model time resolution systematics dominant for Γ_s and $\Delta\Gamma_s$

	ϕ_s [rad]	$\Delta\Gamma_s$ [ps^{-1}]	Γ_s [ps^{-1}]	$\|A_{\|\|}(0)\|^2$	$\|A_0(0)\|^2$	$\|A_s(0)\|^2$	$\delta_\perp$ [rad]	$\delta_{\|\|}$ [rad]	$\delta_\perp - \delta_s$ [rad]
Tagging	$\boxed{0.0174}$	0.0004	0.0003	0.0002	0.0002	0.0023	0.0191	0.0221	0.0022
Acceptance	0.0007	$< 10^{-4}$	$< 10^{-4}$	0.0008	0.0007	$\boxed{0.0024}$	0.0331	0.0140	0.0026
ID Alignment	0.0007	0.0001	0.0005	10^{-4}	10^{-4}	10^{-4}	0.0101	0.0072	10^{-4}
S wave-phase	0.0002	$< 10^{-4}$	$< 10^{-4}$	0.0003	10^{-4}	0.0003	0.0112	0.0212	$\boxed{0.0083}$
Background Angles Model:									
Choice of fit function	0.0018	0.0008	$< 10^{-4}$	$\boxed{0.0014}$	0.0007	0.0002	$\boxed{0.0850}$	$\boxed{0.1920}$	0.0018
Choice of P_T bins	0.0013	0.0005	$< 10^{-4}$	0.0004	0.0005	0.0012	0.0015	0.0072	0.0010
Choice of mass interval	0.0004	0.0001	0.0001	0.0003	0.0003	0.0013	0.0044	0.0074	0.0023
Dedicated Backgrounds:									
B_d^0	0.0023	0.0011	$< 10^{-4}$	0.0002	$\boxed{0.0031}$	0.0014	0.0102	0.0232	0.0021
λ_b	0.0016	0.0004	0.0002	0.0005	0.0012	0.0018	0.0138	0.0295	0.0008
Fit Model:									
Time res. sig frac	0.0014	0.0011	$< 10^{-4}$	0.0005	0.0006	0.0006	0.0120	0.0297	0.0004
Time res. P_T bins	0.0033	$\boxed{0.\ 0014}$	$\boxed{0.001}$	10^{-4}	10^{-4}	0.0005	0.0062	0.0052	0.0011
TOTAL	**0.018**	**0.002**	**0.001**	**0.002**	**0.004**	**0.004**	**0.097**	**0.201**	**0.010**

Combination of Run 1 - Run 2 results

- A Best Linear Unbiased Estimate (BLUE) combination is performed to combine the current result with the Run 1 measurement
- The BLUE combination uses the measured values and uncertainties of the parameters as well as the correlations between them

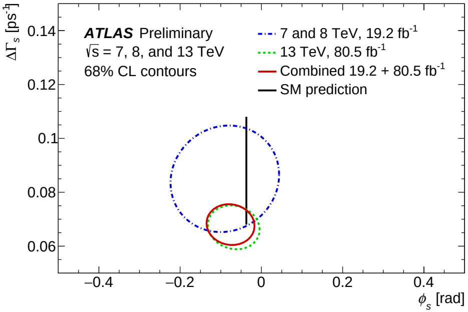

	13 TeV data			Combined 13 TeV with 7 TeV and 8 TeV data		
Par	Value	Stat	Syst	Value	Stat	Syst
ϕ_s[rad]	−0.068	0.038	0.018	−0.076	0.034	0.019
$\Delta\Gamma_s$[ps^{-1}]	0.067	0.005	0.002	0.068	0.004	0.003
Γ_s[ps^{-1}]	0.669	0.001	0.001	0.669	0.001	0.001
$\lvert A_\parallel(0)\rvert^2$	0.219	0.002	0.002	0.220	0.002	0.002
$\lvert A_0(0)\rvert^2$	0.517	0.001	0.004	0.517	0.001	0.004
$\lvert A_S\rvert^2$	0.046	0.003	0.004	0.043	0.004	0.004
$\delta_\perp$ [rad]	2.946	0.101	0.097	3.075	0.096	0.091
$\delta_\parallel$ [rad]	3.267	0.082	0.201	3.295	0.079	0.202
$\delta_\perp - \delta_S$ [rad][*]	−0.220	0.037	0.010	−0.216	0.037	0.010

[*] A correction due to $m(K^+K^-)$ dependence of phase difference between S and P waves is applied in the current analysis, but was missing in the Run 1 analysis. Therefore the Run 1 value of $\delta_\perp - \delta_S$ is not used.

Updated overview and the Conclusion

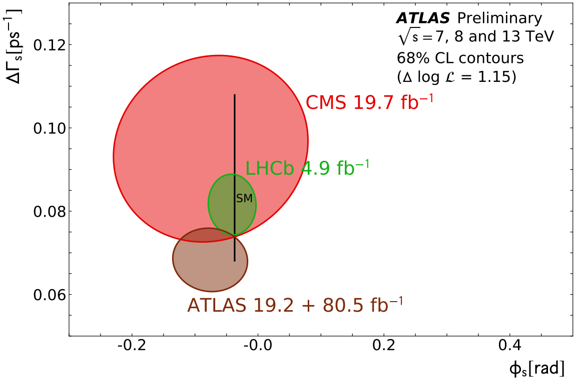

Current results on ϕ_s from LHC

	ϕ_s [rad]
LHC Combined Run 1	-0.021 ± 0.031
ATLAS Run 1, JHEP08, 147	-0.090 ± 0.078 (stat) $\pm$ 0.041 (syst)
CMS Run 1, Phys.Lett. B757, 97	-0.075 ± 0.097 (stat) $\pm$ 0.031 (syst)
LHCb 2015/16 $\oplus$ Run 1, arXiv:1906.08356	-0.080 ± 0.032
ATLAS 2015/16/17 (80.5 fb^{-1}) $\oplus$ Run 1 (19.2 fb^{-1})	-0.076 ± 0.034 (stat) $\pm$ 0.019 (syst)
HFLAV Combined	-0.055 ± 0.021

Backup slides

Probability density functions

$$\ln \mathcal{L} = \sum_{i=1}^{N} \{ w_i \cdot \ln(f_{\rm s}\mathcal{F}_{\rm s} + f_{\rm s} f_{B^0}\mathcal{F}_{B^0} + f_{\rm s} f_{\Lambda_b}\mathcal{F}_{\Lambda_b} + (1 - f_{\rm s}(1 + f_{B^0} + f_{\Lambda_b}))\mathcal{F}_{\rm bkg} \}$$

Peaking backgrounds

- Contributions from $B_d^0 \to J/\psi K^{*0}$, $B_d^0 \to J/\psi K\pi$ and $\Lambda_b^0 \to J/\psi Kp$
- Shapes of distributions changed due to wrong mass assignment (KK)
- PDFs extracted from MC and then fixed in the main fit
- Fractions calculated from:
  - Efficiencies and acceptance from MC
  - BR from PDG
  - Fragmentation fractions from other measurements

Combinatorial background PDFs

- Mass: exponential + constant
- Time: delta-function and 3 exponentials convolved with per-candidate time resolution
- Angles: Legendre polynomials from sidebands; fixed in the main fit

Signal time-angular PDF

k	$\mathcal{O}^{(k)}(t)$	$g^{(k)}(\theta_T, \psi_T, \phi_T)$
1	$\frac{1}{2}\lvert A_0(0)\rvert^2 \left[(1+\cos\phi_s)\, e^{-\Gamma_{\mathrm{L}}^{(s)} t} + (1-\cos\phi_s)\, e^{-\Gamma_{\mathrm{H}}^{(s)} t} \pm 2e^{-\Gamma_s t} \sin(\Delta m_s t) \sin\phi_s\right]$	$2\cos^2\psi_T(1-\sin^2\theta_T\cos^2\phi_T)$
2	$\frac{1}{2}\lvert A_\parallel(0)\rvert^2 \left[(1+\cos\phi_s)\, e^{-\Gamma_{\mathrm{L}}^{(s)} t} + (1-\cos\phi_s)\, e^{-\Gamma_{\mathrm{H}}^{(s)} t} \pm 2e^{-\Gamma_s t} \sin(\Delta m_s t) \sin\phi_s\right]$	$\sin^2\psi_T(1-\sin^2\theta_T\sin^2\phi_T)$
3	$\frac{1}{2}\lvert A_\perp(0)\rvert^2 \left[(1-\cos\phi_s)\, e^{-\Gamma_{\mathrm{L}}^{(s)} t} + (1+\cos\phi_s)\, e^{-\Gamma_{\mathrm{H}}^{(s)} t} \mp 2e^{-\Gamma_s t} \sin(\Delta m_s t) \sin\phi_s\right]$	$\sin^2\psi_T\sin^2\theta_T$
4	$\frac{1}{2}\lvert A_0(0)\rvert\lvert A_\parallel(0)\rvert \cos\delta_{\parallel}$ $\left[(1+\cos\phi_s)\, e^{-\Gamma_{\mathrm{L}}^{(s)} t} + (1-\cos\phi_s)\, e^{-\Gamma_{\mathrm{H}}^{(s)} t} \pm 2e^{-\Gamma_s t} \sin(\Delta m_s t) \sin\phi_s\right]$	$\frac{1}{\sqrt{2}}\sin 2\psi_T\sin^2\theta_T\sin 2\phi_T$
5	$\lvert A_\parallel(0)\rvert\lvert A_\perp(0)\rvert[\frac{1}{2}(e^{-\Gamma_{\mathrm{L}}^{(s)} t} - e^{-\Gamma_{\mathrm{H}}^{(s)} t})\cos(\delta_\perp - \delta_{\parallel})\sin\phi_s$ $\pm e^{-\Gamma_s t}(\sin(\delta_\perp - \delta_\parallel)\cos(\Delta m_s t) - \cos(\delta_\perp - \delta_\parallel)\cos\phi_s\sin(\Delta m_s t))]$	$-\sin^2\psi_T\sin 2\theta_T\sin\phi_T$
6	$\lvert A_0(0)\rvert\lvert A_\perp(0)\rvert[\frac{1}{2}(e^{-\Gamma_{\mathrm{L}}^{(s)} t} - e^{-\Gamma_{\mathrm{H}}^{(s)} t})\cos\delta_\perp\sin\phi_s$ $\pm e^{-\Gamma_s t}(\sin\delta_\perp\cos(\Delta m_s t) - \cos\delta_\perp\cos\phi_s\sin(\Delta m_s t))]$	$\frac{1}{\sqrt{2}}\sin 2\psi_T\sin 2\theta_T\cos\phi_T$
7	$\frac{1}{2}\lvert A_S(0)\rvert^2 \left[(1-\cos\phi_s)\, e^{-\Gamma_{\mathrm{L}}^{(s)} t} + (1+\cos\phi_s)\, e^{-\Gamma_{\mathrm{H}}^{(s)} t} \mp 2e^{-\Gamma_s t} \sin(\Delta m_s t) \sin\phi_s\right]$	$\frac{2}{3}\left(1-\sin^2\theta_T\cos^2\phi_T\right)$
8	$\alpha\lvert A_S(0)\rvert\lvert A_\parallel(0)\rvert[\frac{1}{2}(e^{-\Gamma_{\mathrm{L}}^{(s)} t} - e^{-\Gamma_{\mathrm{H}}^{(s)} t})\sin(\delta_\parallel - \delta_S)\sin\phi_s$ $\pm e^{-\Gamma_s t}(\cos(\delta_\parallel - \delta_S)\cos(\Delta m_s t) - \sin(\delta_\parallel - \delta_S)\cos\phi_s\sin(\Delta m_s t))]$	$\frac{1}{3}\sqrt{6}\sin\psi_T\sin^2\theta_T\sin 2\phi_T$
9	$\frac{1}{2}\alpha\lvert A_S(0)\rvert\lvert A_\perp(0)\rvert\sin(\delta_\perp - \delta_S)$ $\left[(1-\cos\phi_s)\, e^{-\Gamma_{\mathrm{L}}^{(s)} t} + (1+\cos\phi_s)\, e^{-\Gamma_{\mathrm{H}}^{(s)} t} \mp 2e^{-\Gamma_s t} \sin(\Delta m_s t) \sin\phi_s\right]$	$\frac{1}{3}\sqrt{6}\sin\psi_T\sin 2\theta_T\cos\phi_T$
10	$\alpha\lvert A_0(0)\rvert\lvert A_S(0)\rvert[\frac{1}{2}(e^{-\Gamma_{\mathrm{H}}^{(s)} t} - e^{-\Gamma_{\mathrm{L}}^{(s)} t})\sin\delta_S\sin\phi_s$ $\pm e^{-\Gamma_s t}(\cos\delta_S\cos(\Delta m_s t) + \sin\delta_S\cos\phi_s\sin(\Delta m_s t))]$	$\frac{4}{3}\sqrt{3}\cos\psi_T\left(1-\sin^2\theta_T\cos^2\phi_T\right)$

Performing the calibrations

- Results of Fit provide $N_{B\pm}^{Q=i}$; P(Q|B+) = N(B+|Q) / N(B+)

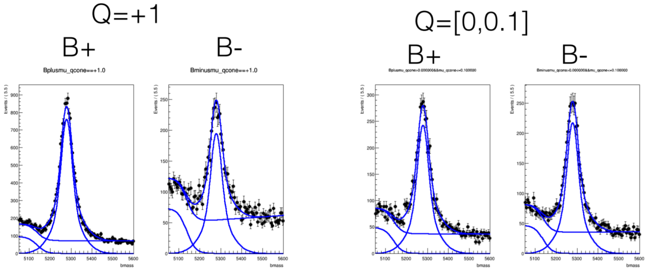

- Calibration curve separated into
  - Continuous and discrete parts
- Converts Q values into a Probability

$$
\begin{aligned}
P(\bar{b}|Q) &= \frac{P(Q|\bar{b})P(\bar{b})}{P(Q|\bar{b})P(\bar{b}) + P(Q|b)P(b)} \\
&= \frac{P(Q|\bar{b})}{P(Q|\bar{b}) + P(Q|b)},
\end{aligned}
$$

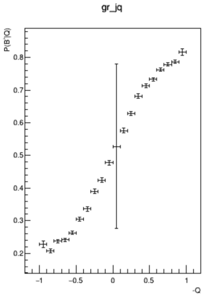

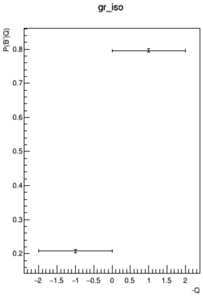

Tag charge distribution and calibration curves

Tight muons

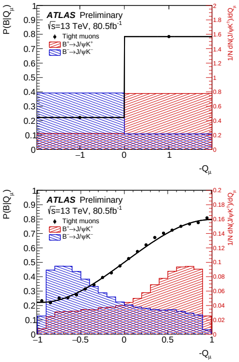

Low-p_{T} muons

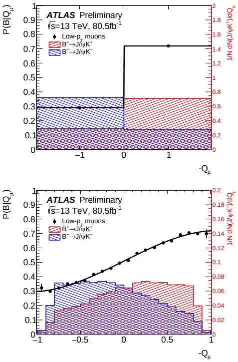

Electrons

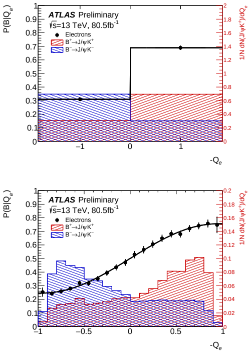

Jets

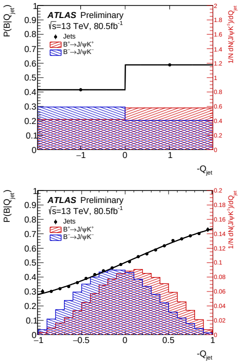

Tag "Punzi" distributions - discrete

- Fraction of tag-charge equal to ±1 in signal and background events

Tag method	Signal		Background	
	f_{+1}	f_{-1}	f_{+1}	f_{-1}
Tight μ	0.069 ± 0.003	0.075 ± 0.003	0.047 ± 0.001	0.049 ± 0.001
Electron	0.20 ± 0.01	0.19 ± 0.01	0.168 ± 0.002	0.173 ± 0.002
Low-pt μ	0.109 ± 0.005	0.117 ± 0.005	0.070 ± 0.001	0.076 ± 0.001
Jets	0.0451 ± 0.0015	0.0458 ± 0.0016	0.0376 ± 0.0003	0.0386 ± 0.0003

- Fraction of tag-methods in signal and background events

Tag method	Signal	Background
Tight μ	0.0400 ± 0.0006	0.0316 ± 0.0001
Electron	0.0187 ± 0.0004	0.0148 ± 0.0001
Low-pT μ	0.0291 ± 0.0005	0.0264 ± 0.0001
Jets	0.144 ± 0.001	0.1196 ± 0.0002
Untagged	0.767 ± 0.003	0.8077 ± 0.0005

Systematic uncertainties

- Flavour tagging systematics:
  - calibration function (tag probability vs. tag charge)
  - pile-up dependence (calibration for three N_{PV} bins)
  - variation of tag probability and tag method "Punzi" terms (functions, histograms)
  - stat. uncertainty due to $B^{\pm} \to J/\psi K^{\pm}$ data sample included in overall stat. err.
- Angular acceptance (binned fit of MC) by changing the bin widths and central values
- Inner detector alignment: Residual misalignment affects tracks impact parameter, effect in fit results in systematics
- S-wave phase by varying correction factor α that accounts for mass-dependence of phase difference between S and P waves
- Background angles model varying Legendre polynomials describing sidebands data:
  - their degree
  - B-p_{T} dependence (binning)
  - size of B_s^0 mass sidebands
- Contributions from peaking backgrounds $B_d^0 \to J/\psi K^{*0}$, $B_d^0 \to J/\psi K\pi$ and $\Lambda_b^0 \to J/\psi Kp$, accounting for:
  - production fraction uncertainties
  - uncertainties in modeling of decay angles (including S/P wave interference)
  - uncertainties of fit-function describing the mass-time-angular PDFs
- Signal fit model:
  - adding second mass scale factor
  - varying B-p_{T} binning (decay time per-candidate errors sensitive to that)
  - varying signal fraction when determining the decay time "Punzi" terms